Journal of Biomedical Optics

BiomedicalOptics.SPIEDigitalLibrary.org

Systemic low-frequency oscillations observed in the periphery of healthy human subjects

Yingwei Li
Haibing Zhang
Meiling Yu
Weiwei Yu
Blaise deB Frederick
Yunjie Tong

SPIE.

Yingwei Li, Haibing Zhang, Meiling Yu, Weiwei Yu, Blaise deB Frederick, Yunjie Tong, "Systemic low-frequency oscillations observed in the periphery of healthy human subjects," *J. Biomed. Opt.* **23**(5), 057001 (2018), doi: 10.1117/1.JBO.23.5.057001.

Systemic low-frequency oscillations observed in the periphery of healthy human subjects

Yingwei Li,[a,b,c] Haibing Zhang,[a] Meiling Yu,[a] Weiwei Yu,[a] Blaise deB Frederick,[b,c] and Yunjie Tong[d,*]
[a]Yanshan University, School of Information Science and Engineering, Hebei, China
[b]McLean Hospital, Brain Imaging Center, Belmont, Massachusetts, United States
[c]Harvard Medical School, Department of Psychiatry, Boston, Massachusetts, United States
[d]Purdue University, Weldon School of Biomedical Engineering, West Lafayette, Indiana, United States

Abstract. This study investigated the relationships of systemic low-frequency oscillations (sLFOs) measured at different peripheral sites in resting state, during passive leg raising (PLR), and during a paced breathing (PB) test. Twenty-five healthy subjects (21 to 57 years old; males: 13 and females: 12) were recruited for these experiments. During the experiments, the fluctuations of oxyhemoglobin concentration were measured at six peripheral sites (left and right toes, fingertips, and earlobes) using a multichannel near-infrared spectroscopy instrument developed by our group. We applied cross-correlation and frequency component analyses on the data. The results showed that the sLFO signals in the symmetric peripheral sites were highly correlated, with time delays close to zero, whereas the correlation coefficients decreased between the sLFO signals of asymmetric sites, with delays up to several seconds. Furthermore, in PLR/PB tests, we found that PB caused wider and more robust changes in hemoglobin concentrations at peripheral sites compared to PLR. Among six peripheral sites, earlobes were the most sensitive to these perturbations, followed by fingertips, and then toes. Lastly, we showed that the perturbation signals may have different coupling mechanisms than the sLFO signals. The study deepened our understanding of the sLFO signals and establishes baseline measures for developing perfusion biomarkers to assess peripheral vascular integrity.
[DOI: 10.1117/1.JBO.23.5.057001]

Keywords: near-infrared spectroscopy; systemic low-frequency oscillations; peripheries; resting state; passive leg raising; paced breathing; peripheral artery disease.

Paper 170552RR received Aug. 27, 2017; accepted for publication Apr. 9, 2018; published online May 4, 2018.

1 Introduction

Low-frequency oscillations (LFOs: 0.01 to 0.15 Hz) are slow, spontaneous variations in hemodynamic parameters commonly observed in resting-state (RS) functional studies by functional near-infrared spectroscopy (fNIRS) and functional MRI (fMRI).[1–11] In the brain, some of these LFOs reflect neuronal activations indirectly through neurovascular coupling,[12] which is the basis of these functional studies. However, a significant fraction of the LFO signals is related to physiological fluctuations.[13–15] To distinguish them from the neuronal LFOs, we refer to these physiological fluctuations (~0.1 Hz) as systemic LFOs (sLFOs). The origins and functions of these sLFOs are complex and not fully understood.[16] They have been attributed to respiration, Mayer waves, vasomotion, and CO_2 fluctuations in the blood. Moreover, studies have shown that a significant change in the power of LFOs (in oxyhemoglobin concentration) was observed between different postures, such as standing versus supine or sitting versus supine.[17] These spontaneous oscillations have been measured by fNIRS (e.g., in the prefrontal region) to study dynamic cerebral autoregulation[18,19] corresponding to fluctuations in arterial blood pressure (ABP by plethysmograph) and cerebral blood flow velocity (CBFV by transcranial Doppler ultrasound). However, few studies have focused on the presence of these spontaneous oscillations in the periphery.

In our previous studies, we found that these sLFO signals could also be observed in peripheral regions, such as earlobes, fingertips, and toes. In a previous concurrent fMRI/NIRS study,[11] we acquired RS fMRI data on healthy subjects while simultaneously recording their sLFO signals in the fingertips and toes using NIRS. The correlations between the blood-oxygen-level dependent fMRI signals in the brain and oxyhemoglobin concentration changes ($\Delta[HbO]$) in the periphery are significant. This indicates that this is the same sLFO signal observed at multiple locations. Furthermore, we observed that the sLFO from fingertip always leads those from the toe by a few seconds. This is consistent with the hypothesis that these sLFOs likely originate in the heart/lung system and travel with the blood to different parts of the body. Due to the shorter vascular path to the fingertip, the sLFOs always reach the fingertips earlier than the toes.

This is an intriguing and useful phenomenon for the following reasons. First, since these sLFOs are intrinsic spontaneous oscillations, they can be treated as natural "tags" on the flowing blood. By comparing the arrival times and the intensity of the signal at different peripheral locations, we can assess vascular integrity. Second, these peripheral sites are ideal for NIRS measurements. Commercial pulse plethysmographs are widely available for earlobe and fingertip measurements. With simple modification, they can be easily adapted to measure the frequencies of interest and to record from the toes with little setup time.

*Address all correspondence to: Yunjie Tong, E-mail: tong61@purdue.edu

1083-3668/2018/$25.00 © 2018 SPIE

Last and more importantly, all these peripheral sites have simple tissue structure, which allows immediate and almost direct interaction between photons and the blood vessels, leading to superior signal-to-noise ratio (SNR) compared to functional brain studies, where light must penetrate multiple layers of highly scattering mediums (skin and skull) before reaching the cortex.

In this study, we sought to extend the research on these sLFOs in the periphery. This study had two goals: (1) to determine the correlation and time delays of sLFOs measured at symmetric and asymmetric peripheral sites among healthy subjects. The results can be used as normative baseline values when assessing populations with vascular disease in the future. (2) To understand how some perturbations modulate sLFOs, and how these modulated LFO signals "propagate" to the other parts of the periphery. The goal is to identify some perturbation as a "stress" test for the peripheral vasculature. With it, some "hidden" dysfunction may be exposed for early detection. In this study, we used simplified versions of two well-known tasks [paced breathing (PB) and passive leg raising (PLR)]. The differences between these tasks are as follows. (1) PB is considered as a perturbation of the "central" system (i.e., heart/lung). This perturbation might affect the entire periphery equally, either through blood circulation (i.e., CO_2 modulation in the blood) or by an ABP effect. (2) PLR causes regional perturbation, which will be reflected in the corresponding leg (or toe). However, its effect on the other peripheral sites is less known, as it is likely primarily a hydrostatic pressure change.

The long-term goal of this study is to develop natural perfusion biomarkers (i.e., sLFOs correlation parameters) as well as some simple "stress tests" to easily assess peripheral vascular integrity. One of these applications can be early detection and diagnose of peripheral artery disease (PAD). PAD is a narrowing of arteries in the arm, and most commonly in the leg. It affects millions of Americans, especially among the elderly and in patients with diabetes. Normally, PAD affects one leg more than the other, leading to asymmetric flow patterns to the periphery. We predict that the time of LFOs observed at symmetric peripheral site, such as two toes, will be different in PAD patients, and larger delays will be correlated with more severe symptoms.

2 Materials and Methods

2.1 *Multichannel Research Oximeter*

Commercial plethysmographs (i.e., pulse oximeters) are simple NIRS instruments used to measure time-varying hemodynamic parameters corresponding to heart beat. In these devices, sLFO signals are considered a nuisance and are filtered out to more easily calculate pulse rate and oxygen saturation. To assess the signals with wider bandwidth (i.e., sLFOs), we have to develop our own multichannel NIRS oximeter [multichannel research oximeter (MRO)] based on standard photoplethysmograph hardware with modified acquisition software.[20] The assembled device is shown in Fig. 1(a). It has seven NIRS channels and one electrocardiography channel with a flat frequency response from DC to 31.25 Hz. The core of each NIRS channel is an Olimex MOD-PULSE pulse oximeter development board (Olimex, Ltd., Plovdiva Bulgaria). The details of the device can be found in our previous publication.[20] We used the following channel designations throughout the paper: LE, left earlobe; RE, right earlobe; LF, left finger; RF, right finger; LT, left toe; and RT, right toe.

2.2 *Protocols*

We recruited 25 healthy subjects, aged between 21 and 57 years old (males: 13 and females: 12). The Institutional Review Board at McLean Hospital approved the protocol, and the informed consent forms were obtained from all subjects before their participation in the study. Six Nellcor type pulse oximeter probes were placed over the subject's two earlobes, two index fingers, and two second toes as shown in Fig. 1(b). The NIRS sampling rate of 31.25 Hz allows one to fully sample cardiac, respiratory,

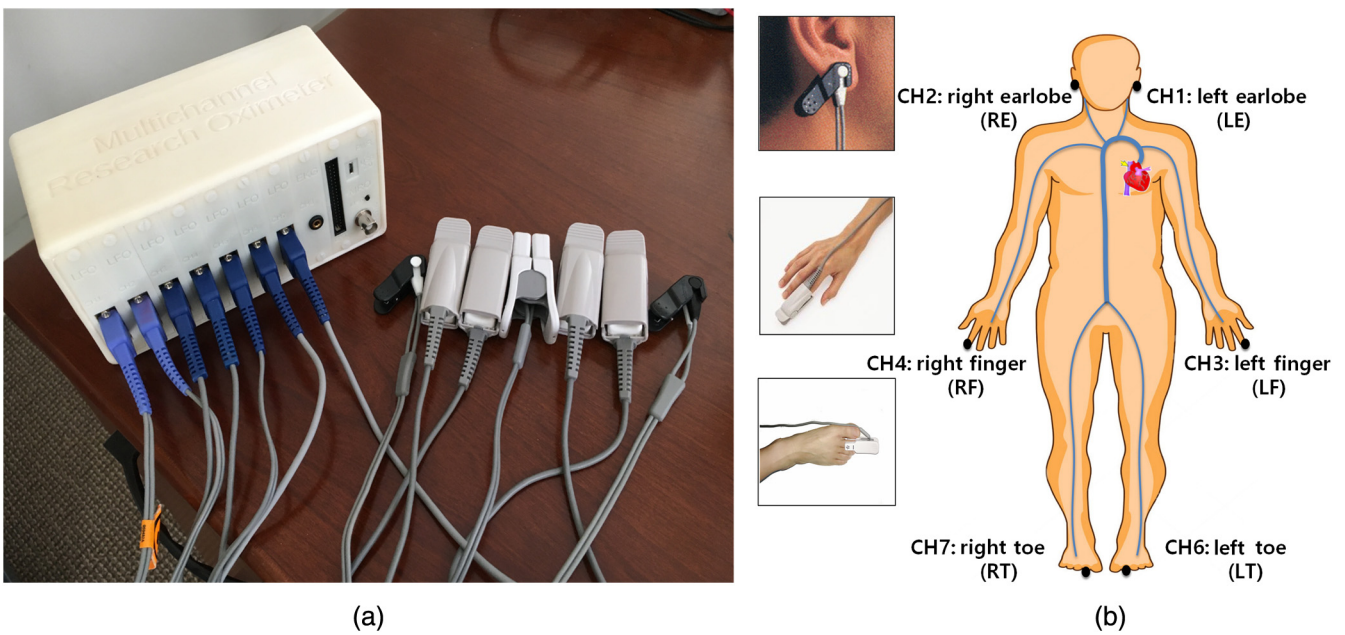

Fig. 1 The equipment and experimental setup. (a) MRO developed by our group, with Nellcor type pulse oximeter probes for fingertip, toe, and earlobe. (b) The placement of the NIRS probes (i.e., over the two earlobes, two index fingers, and two toes) on the subject.

and sLFOs waveforms without aliasing. The sLFOs at multiple peripheral sites were measured simultaneously by the MRO while the subjects were in supine position on a comfortable bed with eyes open in a quiet and warm room. The experiments started with a 10-min RS recording. In the next 10-min period, the subject's left leg was lifted periodically using a flat board placed underneath the leg, by an experimenter in the following repeating pattern: (1) lift the left leg to a height of 50 cm (from the heel to the bed; the angle with the ground was approximate 30 deg to 35 deg) over ~1 s, (2) hold the leg in this position for ~9 s, (3) lower the leg onto the bed in 1 s, and (4) rest for 9 s. After 2 min, the subject had 1 min of rest, and then the cycle was repeated. Three lifting–resting blocks were used in the experiment. It is important to note that the flat board used in the experiment kept even the pressure on the leg (i.e., keep the circulation) and reduced motion artifacts. Last, we asked the subject to do a PB procedure according to a cue shown on a computer screen. In detail, subjects were asked to keep supine position while watching the screen through a 45-deg mirror. After 1-min rest, regular PB was performed at the rate of 6/min (0.1 Hz) for 2 min. A total of three resting–breathing trials were carried out. The whole process lasted for 10 min. We did not measure the tidal volumes in PB. To avoid other potential confounds of PB, such as hypocapnia, the subjects were carefully instructed to breathe with low tidal volumes.

2.3 *Methods for Data Analysis*

Each pair of raw NIRS time courses (660- and 920-nm data) were converted into three time courses representing Δ[HbO], Δ[Hb], and total hemoglobin concentration change (Δ[tHb]) using the modified Beer–Lambert law.[21,22] For the differential path length factors, we used published values of 6.51 at 660 nm and 5.86 at 920 nm. The low-frequency component (0.01 to 0.15 Hz) of Δ[HbO], Δ[Hb], and Δ[tHb] was obtained using a digital zero-delay bandpass filter in MATLAB™, which is a Butterworth filter (order 3), with lower cutoff frequency of 0.01 Hz and higher cutoff frequency of 0.15 Hz. Due to high SNR, we used Δ[HbO] to calculate the main results of the study. However, we also discussed the results of Δ[Hb] in the discussion.

To understand the spectral content of the signals, we calculated the power spectral density (PSD) of the Δ[HbO] signal collected at the peripheral sites in: (1) RS, (2) PLR, and (3) PB acquisitions. For RS, we wanted to explore the differences between symmetric sites and asymmetric sites in PSD. For PLR and PB, we wanted to know the presences of 0.05-Hz peak in the PSD of PLR (or 0.1-Hz peak in PB) in all sites. Because these peaks were sometimes difficult to identify, we established simple, objective criteria to define the "observability." First, in the PSD of PLR, the 0.05-Hz peak must be in the range of 0.048 to 0.052 Hz (in PB, the range was 0.09 to 0.11 Hz). Second, after removing DC and very slow drifts (using the bandpass filter of 0.01 to 0.15 Hz, see Sec. 2.2), the amplitude of the identified peak at 0.05 and/or 0.1 Hz needs to be larger than 10% of the largest peak in the whole power spectrum. In each peripheral site, every trial (total of 75 trials in PLR or PB) was scored for signal observability (1 if observed, 0 if not).

The maximum cross-correlation coefficients (MCCCs) between the sLFOs in different sites were calculated using the MATLAB™ "xcorr" function, and the corresponding time delays were found. We restricted the search range of time delays

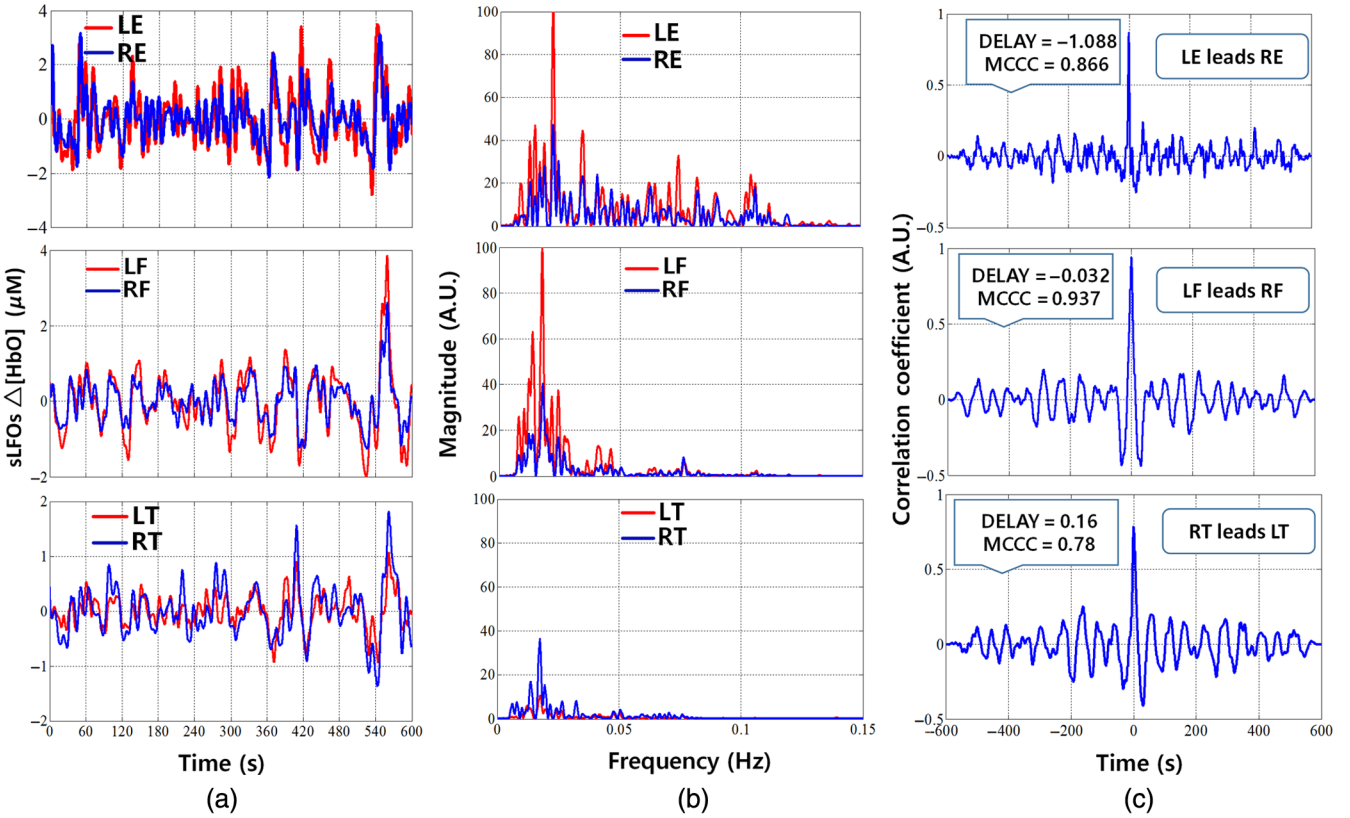

Fig. 2 Time-frequency and correlation results in symmetric peripheral sites in RS for subject 6. (a) Time courses of sLFOs, (b) corresponding PSD of sLFOs, and (c) corresponding cross-correlation plots.

to be ±20 s, according to the global circulation time.[23] When the magnitude of the time delay between the two signals exceeded 20 s or MCCCs were lower than 0.3 (the spurious correlation threshold), the measurement was discarded. Last, to assess the characteristics of the propagation of the perturbations in both PLR and PB tasks at their specific frequency (PLR: 0.05 Hz, PB: 0.1 Hz), we employed the cross PSD (CPSD in MATLAB™) to calculate the phase difference (reflecting the time delays) among these peripheral sites (details in the Appendix A).[24]

3 Results

3.1 *sLFOs in Peripheral Sites in Resting State*

To the best of our knowledge, this is the first concurrent NIRS study establishing the relationship between the sLFOs component of Δ[HbO] in the bilateral extremities in the periphery. Example sLFO signals (i.e., subject 2) from symmetric sites (finger, toes, and earlobes) are shown in Fig. 2(a). The power spectra are shown in Fig. 2(b), and the cross-correlation plots are shown in Fig. 2(c). From these plots, we have the following observations. The sLFO signals from symmetric peripheral sites are highly correlated (>0.7) with small time delays (<2 s). This can also be seen in the power spectra plots, where the signals from symmetric sites have largely overlapping PSD. However, the sLFO signals from different peripheral sites are less similar. In Fig. 2(b), we can see that even though all the sLFO signals share the similar low-frequency components (<0.04 Hz), their high-frequency components varied with earlobe data having the widest power spectrum, that is, up to 0.12 Hz.

The relationship between sLFO signals of asymmetric sites is shown in Fig. 3. Apparently, there are larger differences between these signals in both time and frequency domains [Figs. 3(a) and 3(b)]. For example, sLFO signal of the LE has the spectral range from 0.01 to 0.12 Hz. On the contrary, the sLFO signal power from RF is concentrated at 0.02 Hz. Moreover, the MCCCs calculated between these asymmetric sites are lower with much larger time delays [as in Fig. 3(c)] compared to the values between symmetric pairs of sites.

The MCCCs and delay results for all the subjects are summarized in Fig. 4. The blue rectangle represents the central data points (interquartile range), and we can observe the mean (black line) and standard deviation from the light-gray regions at the same time. The red line at the center represents the median. In Fig. 4, we see that: (1) MCCCs of sLFOs between left and right symmetric sites were very high (LE-RE: 0.74 ± 0.14, LF-RF: 0.92 ± 0.08, and LT-RT: 0.89 ± 0.06) with delays close to zero (LE-RE: -0.19 ± 0.82 s, LF-RF: 0.07 ± 0.74 s, and LT-RT: 0.61 ± 0.87 s). (2) The MCCCs dropped to 0.6 when comparing data between fingers and toes, and delays had also increased to ~ -6 s. The sLFO signals of the fingers always lead the signals of the toes, regardless of the site (left or right). (3) The MCCCs dropped further to 0.45 when comparing the data of earlobes and fingers, with averaged delays of ~ -4 s. The sLFO signals from the ears lead the signals from the fingertip.

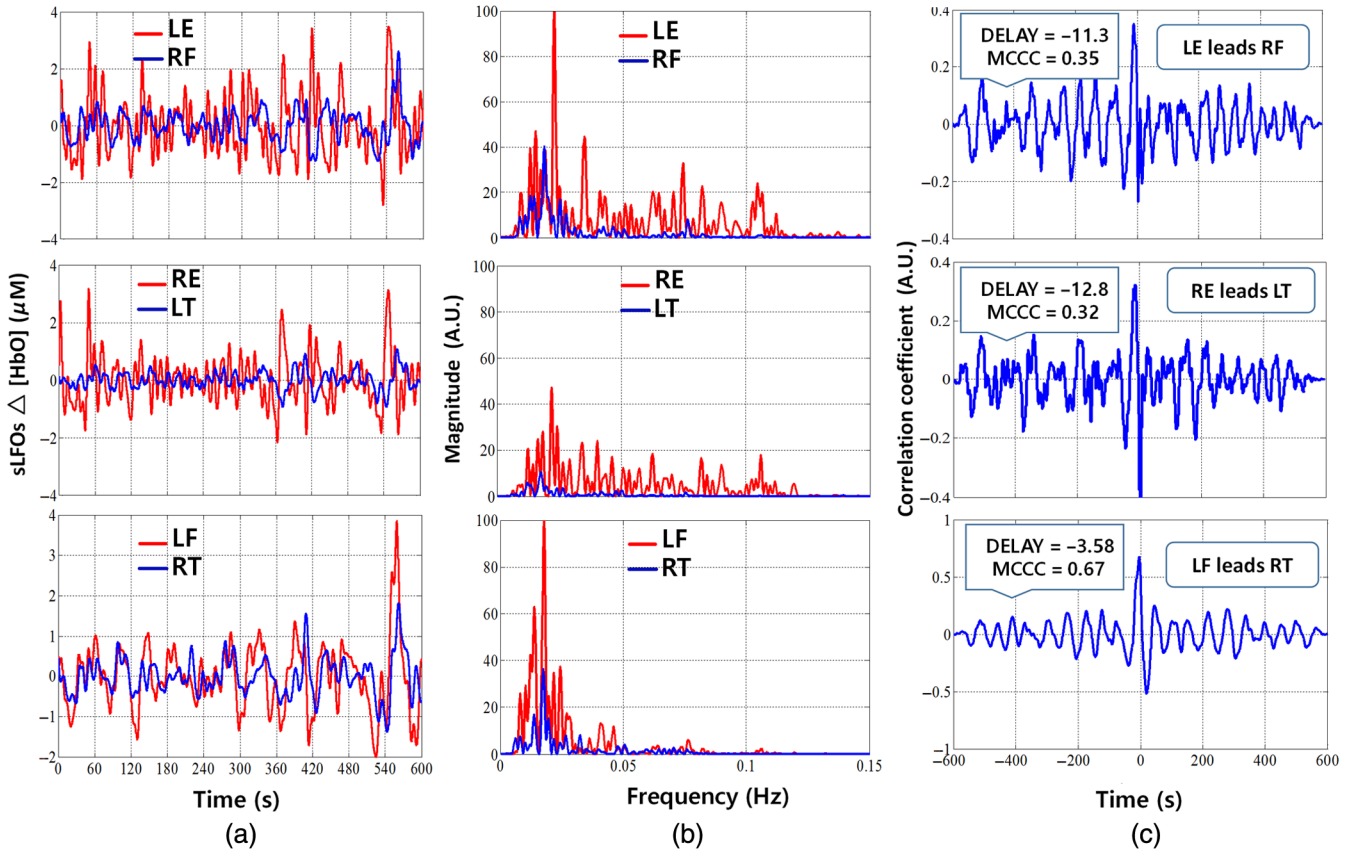

Fig. 3 Time-frequency and correlation results in asymmetric peripheral sites in RS for subject 2. (a) Temporal trace of sLFOs, (b) corresponding PSD of sLFOs, and (c) corresponding cross-correlation plots.

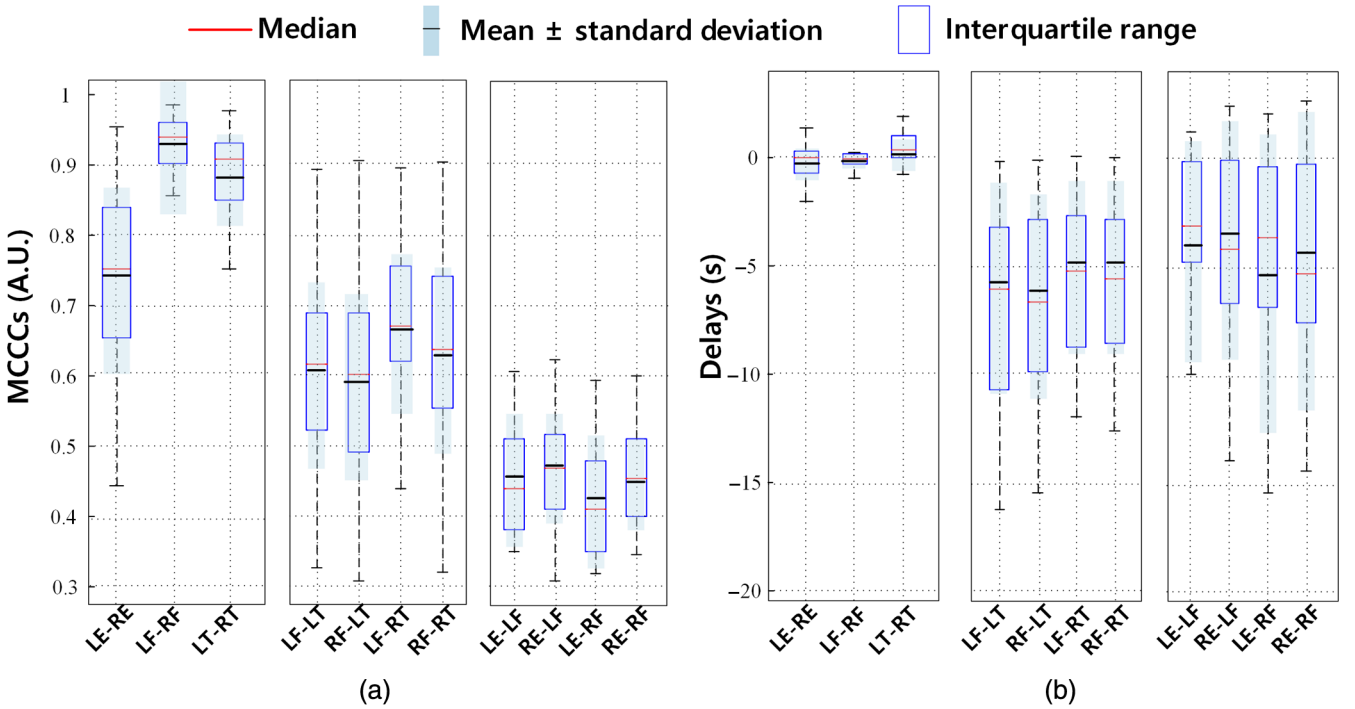

Fig. 4 Statistical results of (a) MCCCs and (b) delays among 25 people in RS.

3.2 *sLFOs at Peripheral Sites During Passive Leg Raising*

Two example results of PLR are shown in Figs. 5(a) and 5(b). The shaded areas (0 to 10 s, 20 to 30 s, 40 to 50 s, 60 to 70 s, 80 to 90 s, and 100 to 110 s) represent the time blocks during which the leg was lifted. When we lifted the left leg, the amplitude of sLFOs from left toes decreased. When we put the left leg down, the amplitude recovered. These changes measured at the left toes were consistent among all the subjects (see Table 1). However, for subject 2, the periodic signals related to PLR were also observed at all the other peripheral sites [Fig. 5(a)], which is confirmed by the spectra plots on the right. On the contrary, in subject 6 [Fig. 5(b)], the PLR-related signals were not as visible in LE and RE. In most subjects, we observe PLR-related signals in some of the peripheral sites. The detailed summary can be found in Table 1, which shows that the PLR signal originating at left leg can "appear" at other peripheral sites with uneven distributions, such as that it can be detected in ~50% of the trials at the earlobes, in 30% to 40% of the trials at the fingertips, and in 24% of the trials at the right toe.

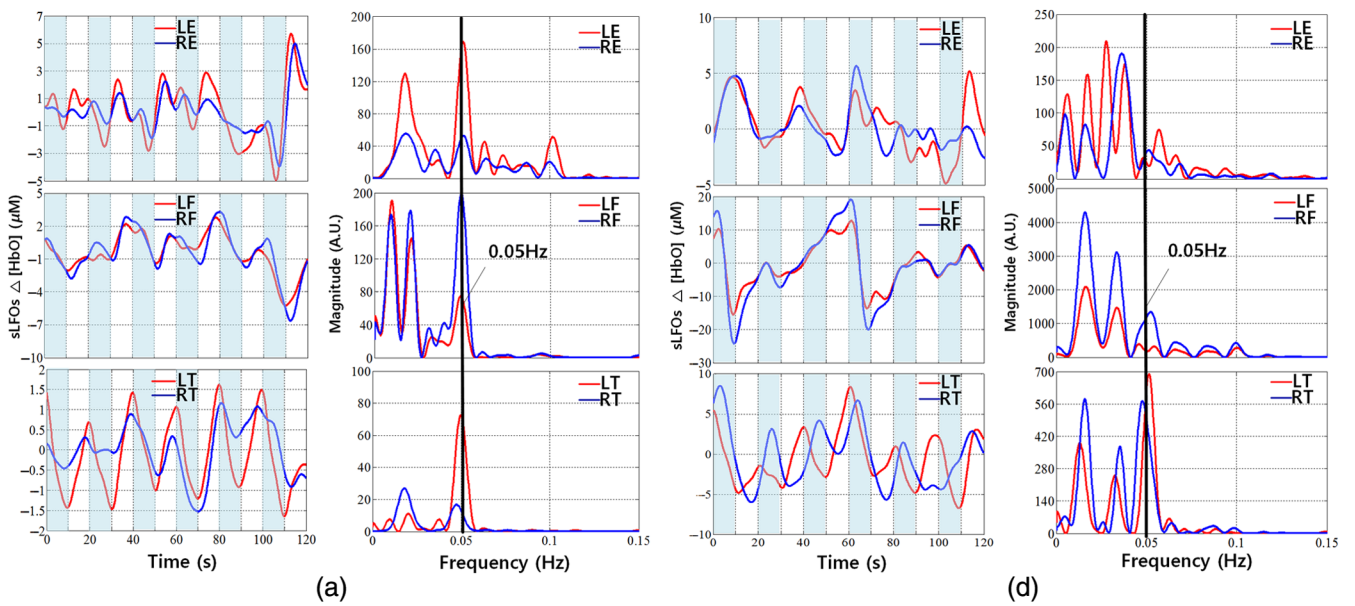

Fig. 5 Time courses and corresponding PSDs of sLFOs at different peripheral sites during PLR (shaded areas represent the periods of leg lifting) for subject 2 in (a) and subject 6 in (b).

Table 1 The number of epochs in which PLR/PB signals can be observed at different peripheral sites during three experimental periods in 25 subjects.

Observability	Value	LE	RE	LF	RF	LT	RT
PLR	Numbers (out of 75 trials)	42	41	32	23	74	18
	Percentages	56	54.67	42.67	30.67	98.67	24
PB	Numbers (out of 75 trials)	68	70	61	58	53	51
	Percentages	90.67	93.33	81	77.33	70.67	68

3.3 *sLFOs at Peripheral Sites at Paced Breathing*

Similar results were observed in PB. Two example results of PB are shown in Figs. 6(a) and 6(b). The shaded areas represent the periods of breath-in during PB. As in PLR, these two subjects represented two extreme cases. In subject 2, the 0.1-Hz PB signals were found at all sites, with small time delays between the symmetric peripheral sites [Fig. 6(a)]. However, in subject 6, the PB frequency only shows up in the signals recorded at earlobes [Fig. 6(b)]. Detailed information can be found in Table 1, which shows that (1) unlike PLR, PB signals are much more easily detected at the peripheral sites than those of PLR (at all sites). For instance, we detected PB signal in about 90% of the earlobes trials and in 70% to 80% of the fingertip and toe trials. (2) Like PLR, the peripheral site that is most likely to detect the signal is the earlobe (>90% of the trials).

4 Discussion

4.1 *sLFOs Observed at Symmetric Peripheral Sites*

sLFO signals were successfully recorded at six peripheral sites with very high signal quality for all 25 subjects. Between the symmetric peripheral sites, we found the following characteristics. First, the sLFO signals have a high degree of similarity. This can be seen in Fig. 2(a) for one example subject and in Fig. 4 for the group results. The MCCCs are high (>0.7, even the lowest: LE-RE: 0.74 ± 0.14) between the sLFOs measured at the symmetric parts, especially, between two toes and two fingertips are around 0.9 (LF-RF: 0.92 ± 0.08 and LT-RT: 0.89 ± 0.06). This is further confirmed by the Fourier transform (FT) in Fig. 2(b), where we observe that two symmetric peripheral sites have similar power spectra in the sLFOs band. Second, there are almost no time delays detected between the sLFOs recorded at pairs of symmetric peripheral sites. From Fig. 4(b), we can see that the majority of the time delays of these 25 healthy subjects are under 1 s. This is especially true for the data for the two fingertips (LF-RF: 0.07 ± 0.74 s). These averaged results calculated between symmetric sites are most robust with small standard deviations, which demonstrated the consistency in the underlying physiological phenomena.

Before proceeding to discuss the physiological meaning, we would like to address the possibility that these results may be the result of spurious correlations. As we know, bandpass filtering and selecting the maximum cross correlation over a time range can inflate the apparent significance of correlation results.[25] This is the reason that we show the FT results as well as the cross-correlation plots in Fig. 2. In Fig. 2(b), we can see that the sLFO signals have complex, inharmonic frequency structure, which means that the sLFO signals are aperiodic in most cases. Therefore, they have no "phase," only time delay. This is clearly seen in Fig. 2(c), where the maximum values of the cross correlation are significantly larger than the neighboring negative/positive values. As a result, the corresponding time delays [Fig. 2(c)] can be extracted quite accurately and unambiguously. Moreover, as suggested in a previous study,[25] where random time series were filtered (<0.1 Hz) and cross correlated to assess the impact on p-value, we found that the MCCC has to be larger than 0.28 to achieve 5% in p-value. Thus, in this study, we chose threshold of 0.3 for MCCC (see Sec. 2.3) to prevent spurious correlation. As shown in the previous studies, the sLFO signals

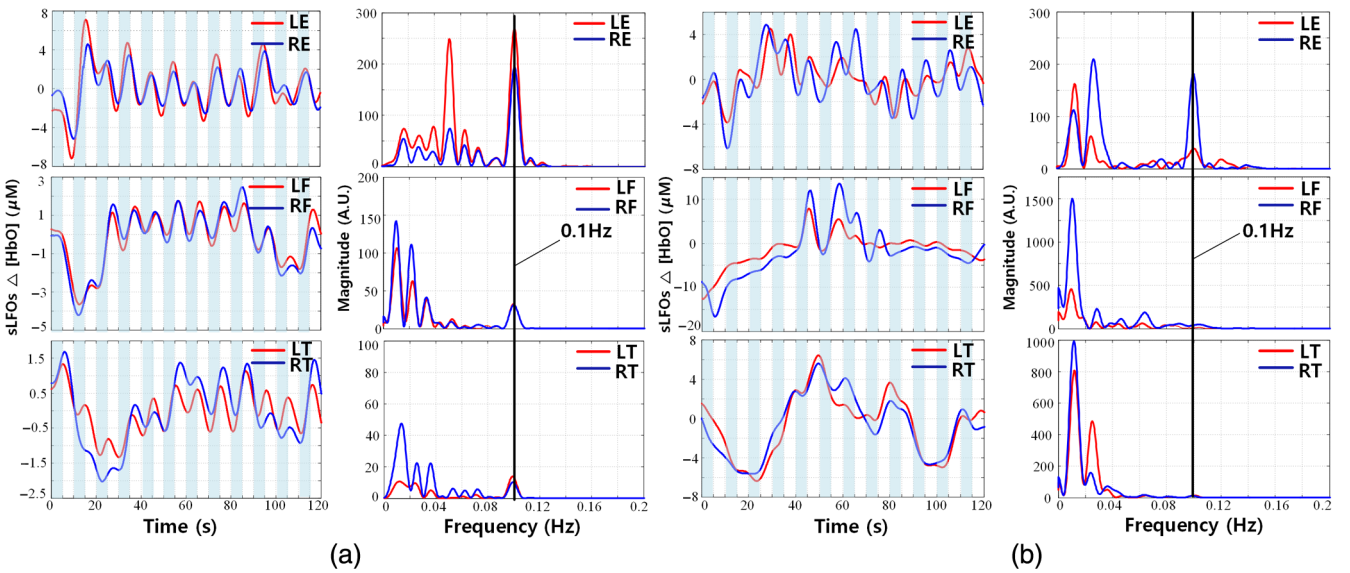

Fig. 6 Time courses and corresponding PSDs of sLFO signals at different peripheral sites in PB (shaded areas represent the periods of breathing in, and blank areas represent the periods of breathing out) for subject 2 in (a) and subject 6 in (b).

are thought to originate in the heart/lung system and flow with the blood throughout the body.[22] As the original sLFOs (from the heart) flow through different paths to different peripheral areas, its features, such as the relative delay and amplitude of the various frequency components, will be modified depending on the specific vascular path it takes. Since the vascular path and distance from the heart to symmetric peripheral sites are similar in healthy subjects, we expect to observe the same sLFOs signal at these sites with extremely small time delays. This is confirmed in Figs. 2 and 4(b), which offer the strongest support of our assumption. Moreover, we also expect that the sLFO signals observed at different peripheral sites should be less similar to each other, with larger time delays. This can be also seen in Fig. 2, where the earlobe sLFO signals are different from those from the toe/fingertip, even though they share some frequency components. Last, we explored the sLFO signals in $\Delta[\mathrm{Hb}]$. It is found that $\Delta[\mathrm{HbO}]$ and $\Delta[\mathrm{Hb}]$ are mostly in-phase at earlobes, whereas the phase difference increases in the fingertips and even more so in the toes. This is reflected in Table 3 in Appendix B, where averaged MCCCs and delays were calculated between $\Delta[\mathrm{HbO}]$ and $\Delta[\mathrm{Hb}]$ at earlobes, fingertips, and toes for all the subjects in RS. From Table 3, we found the averaged MCCC was highest (0.6) in the earlobe and then in the fingertip (0.5). It became negative in the toes (-0.1). This result is very interesting because the phase difference between $\Delta[\mathrm{HbO}]$ and $\Delta[\mathrm{Hb}]$ has been used to assess the underlying physiological parameters and mechanisms,[6,26,27] which might be different at different peripheral sites. However, this is outside the scope of this study, which is focused on the correlations and delays of sLFO at peripheral sites. Based on this, we also calculated the MCCCs and delays between symmetric peripheral sites using $\Delta[\mathrm{Hb}]$. The result was shown in Table 4 in Appendix B. We found similar results (as using $\Delta[\mathrm{HbO}]$) with smaller MCCC values. This confirmed that HbO signal has higher SNR than that of Hb.[28,29]

4.2 *sLFOs Observed at Asymmetric Peripheral Sites*

Figure 3 compares the sLFOs measured at asymmetric peripheral sites, and Figs. 4(a) and 4(b) (middle and right panel) shows the group results. From Fig. 4(a) middle panel, we can see that the MCCCs calculated between sLFOs from fingertips and toes are high (around 0.6) but lower than those between two fingertips or two toes [as in Fig. 4(a) left panel]. The corresponding time delays indicate that the sLFOs at fingertips are generally leading those from the toe by an average of around 6 s. The range of these time delays is wider than those from symmetric peripheral sites. This result matches those from our previous work,[21] where we found sLFOs signal arrived at the fingertips earlier than it reached the toes in an fMRI/fNIRS concurrent study. However, the averaged delay time was different between these two studies (about 3 versus 6 s). Possible contributing factors include: (1) the scanning environment—the previous study was an fMRI/fNIRS concurrent study, where subjects were scanned by fMRI, whereas this study was conducted in a more "relaxed" environment; (2) room temperature—peripheral circulation is affected by ambient temperature, this was not controlled between the studies; and (3) subjects' ages—we have recruited older populations, which may have slower global blood flow. However, when we correlated the age with delays (as show Fig. 9 in Appendix C), no significant correlations were found. More subjects are needed in the future studies. Moreover, we will also control the other factors to determine the effect in the future studies. Figure 4(b) (middle panel), nevertheless, demonstrates the robust delays between the sLFO signals measured at fingertip and toes, regardless of side of the body.

The sLFO signals from the ears are less correlated with those from the fingertips (as in Fig. 4(a) (right panel) with lower averaged MCCCs (around 0.45). The delay time shows leading signals in the earlobe in most cases, which indicates that the sLFOs signal reaches the earlobe ahead of reaching the fingertip. This observation was in line with the fact that the vascular path from heart to earlobe, through the external carotid artery, is shorter than that from the heart to fingertip through the axillary artery. More interestingly, the frequency signature of sLFO signals in earlobes [as shown in Fig. 3(b)] is quite different from those from the fingertips and toes. Significant higher frequency components (>0.04 Hz) can be found in most of signals from the earlobes, while not widely present in those from the fingertips and toes. We do not fully understand the origin of these higher frequency signals in the earlobe (these are not respiratory signals, which are about 0.2 Hz). The complexity of the frequency components, coupled with the high sensitivity to perturbations (i.e., PB/PLR), makes the earlobe signal very interesting and different from the other peripheral signals. It may be that the earlobe signal reflects contributions from facial vascular modulation from the brain.[30] However, the presence of these higher frequency signals in the earlobe affects the accuracy of cross correlation, leading to lower MCCC values and larger error bars when compared with other peripheral signals (even after the thresholding of MCCC >0.3).

4.3 *Perturbation of the LFOs*

4.3.1 *Passive leg lifting test and paced breathing test*

NIRS has been used to study dynamic cerebral autoregulation corresponding to the changes in ABP and CBFV. Spontaneous as well as induced changes in ABP and CBFV have been used in these studies.[31–34] However, little is known about the presence of these spontaneous/induced oscillations in the periphery.

In this study, we tried to use a simplified version of well-known tasks (PLR) to see how mechanical perturbation of one limb would affect the sLFO signal, and if these changes in sLFOs can be detected at other peripheral sites. By transferring a volume of around 300 mL of venous blood from the lower body toward the right heart, PLR creates a fluid challenge. During PLR experiment, we transiently and reversibly increase venous return by shifting venous blood from the legs to the intrathoracic compartment.[23,35] From the temporal traces [in Figs. 5(a) and 5(b), left panel] obtained from lifting the leg (i.e., from left toe), the decline of $\Delta[\mathrm{HbO}]$ was consistently observed during the time of leg lifting due to loss of blood to the lifted site, which recovered after the leg was leveled. Moreover, for many subjects (Table 1), we can reliably observe the corresponding $\Delta[\mathrm{HbO}]$ changes at other peripheral sites. For instance, we can observe the PLR signal (0.05 Hz) at the other leg in 24% of the trials (out of 75), at the fingertips in 30% to 40% of the trials, and at earlobe in 55% of the trials. Similar phenomena were also observed in PB. We found that 0.1-Hz PB signals were even more observable in earlobe ($>90\%$ of trials), followed by fingertip (80%), and then toes (70%). It is known from other studies[36] on autoregulation, which found that both PB (on heart/lung) and thigh-cuff inflation (in the periphery) cause blood pressure changes, leading to observable signals in the brain. However, here we found robust signals in

the earlobe, which is not supposed to be affected by the autoregulation. Moreover, these signals were also found in the fingertips and toes (right toe in PLR). It is of great interest to understand the mechanism of these signals in the periphery (see Sec. 4.3.2).

4.3.2 *Time delays*

Understanding the time delays between these modulated signals at different peripheral sites may shed light on the underlying coupling mechanism. Figure 7 shows the MCCC and time delay results from PLR and PB calculated from different peripheral sites using the same frequency filter (0.01 to 0.15 Hz). We found from the results that (1) at symmetric sites, the delays are still close to 0 s; (2) time delay between finger and toes is about 5 s (finger leading toe) in PLR and 4 s in PB; and (3) the results from earlobe are hard to interpret due to its low MCCC and large variance in delay values on either side of 0. This is likely due to the complicated signals in earlobe as shown in the RS. However, these results are not easy to interpret. For instance, for the peripheral sites where PB (0.1 Hz) and PLR (0.05 Hz) signals are presented, there are still other frequency components (lower). Most of the time, these components were dominant, as shown in Figs. 5 and 6. Therefore, the time delay results might represent the feature of these dominant LFOs, not the signals caused by PB and PLR. This was validated in PB, in which we studied only the signals within the range 0.01 to 0.08 Hz (exclude the PB oscillation at 0.1 Hz). We found the similar results as in Fig. 7 (data not shown). This suggests that there could be two independent oscillations in PLR/PB studies. (1) One is the sLFOs (as studied in RS), which still travels with the blood. The time delay between fingertip and toe in Fig. 7 was likely representing these sLFO signals and showed that the blood flow stayed the same for PLR but increased a little in PB test. (2) The other is PB/PLR signals, "riding" on top of the sLFO signals, which could have very different origin/mechanism and propagation features.

However, there are several problems when assessing only the PB/PLR signals. First, since PB/PLR signals were not present at all sites, this dramatically decreased the sample size, especially in PLR. Second, the PB (0.1 Hz) and PLR (0.05 Hz) signals are too periodic. Third, the PB/PLR could cause signals (i.e., [HbO]) with opposite signs at different sites (see Fig. 6), which could be wrongly interpreted as "delays." Last, it is hard to separate sLFO signals and PLR/PB signals due to the overlapping frequency range (especially in PLR). To address these difficulties, we tried to use CPSD to assess the delay in PB (Fig. 8 in Appendix A) from the fingertips and toes, where 0.1-Hz signal was detected. The results showed that the delays are close to 1 s

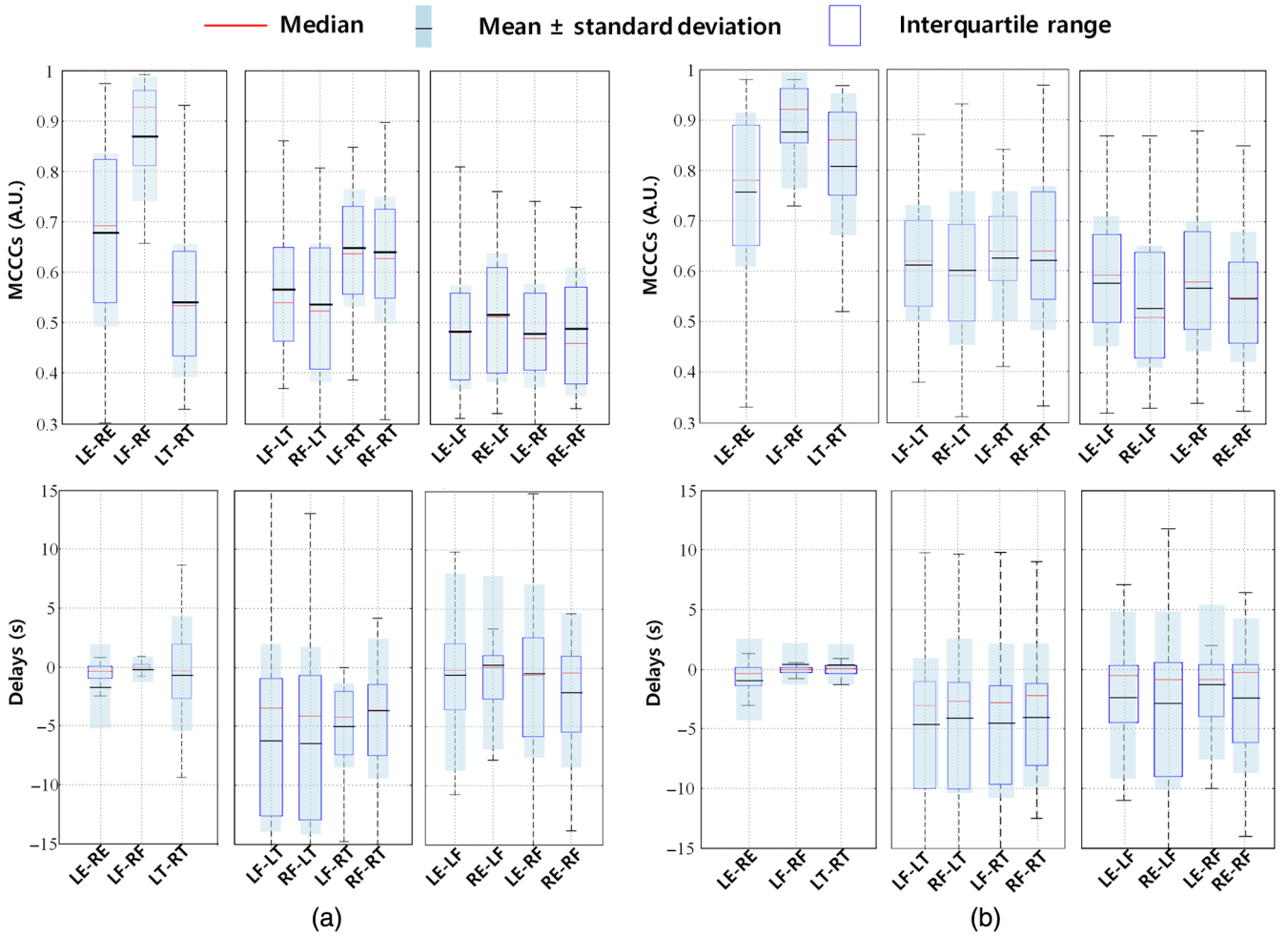

Fig. 7 Statistical results of MCCCs and delays among 25 people in (a) PLR and (b) PB.

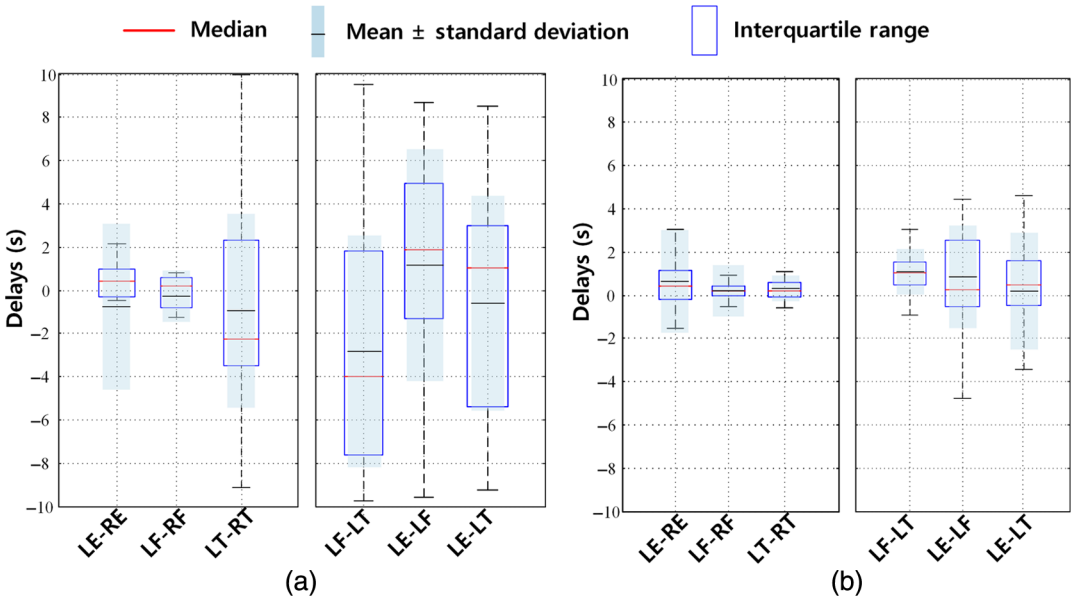

Fig. 8 CPSD results in (a) PLR and (b) PB state among 25 people. The CPSD results are different from cross-correlation results, the negative number means the former signal is lagging the latter one, and the positive number means the former one is leading the latter one.

(signal in fingertip is leading). Therefore, the PB signal did not seem to "propagate" with the blood to the peripheries, which would take seconds. PB does not change the peripheral signals through modulating CO_2 levels in the lung, which then are coupling into the blood. It is likely that PB changes the ABP, which triggers the faster reaction at peripheral sites. Due to small sample size (see the Table 2 in Appendix A) in PLR, it is hard to assess its effects in this study.

Table 2 The data were remained for CPSD calculation to calculate time delays among different sites.

State	LE-RE	LF-RF	LT-RT	LF-LT	LE-LF	LE-LT
PLR	27/75	16/75	16/75	30/75	19/75	42/75
PB	67/75	57/75	44/75	43/75	58/75	49/75

5 Conclusion

We have studied the propagation features of the sLFO signals at different peripheral sites. The high correlation values and corresponding delay times of sLFOs measured between different peripheral sites support the hypothesis that (1) the signals likely originate from the same source (heart/lung system) and (2) they travel with the blood along different vascular paths to reach different part of the body. These features may be used to assess vascular deficit in the patients with peripheral vascular disease. Furthermore, our results showed that simple perturbation, such as PB/PLR, can affect blood signals in remote peripheral sites (especially in the earlobe), which is likely through blood pressure changes. Studying these corresponding signals can shed light on peripheral–central interactions and global feedback/effect of blood pressure changes. Last, peripheral NIRS has been shown to be an effective and accurate tool to measure these changes.

Appendix A: Cross Power Spectral Density Method and Its Results

To assess the feature of propagation of the perturbations in both PLR and PB tasks in their specific frequency (PLR: 0.05 Hz, PB: 0.1 Hz). We employed CPSD function (in MATLAB™) to calculate the phase difference (reflecting the time delays) among these peripheral sites. We set the input signals as LFO component of HbO collected from different sites during PLR and PB test, in which the overlap was set 4096 and the sample frequency was 31.25 Hz. CPSD could be used to calculate phase between different sites in 0.05 Hz in PLR and 0.1 Hz in PB, and we further derived the time delays (in seconds) based on the phase difference.

The results of observability were summarized in Table 2, where it showed that the channel-pairs with observable signals (out of 75 trials). For instance, for LE-RE in PLR, out of 75 trials, we can only observe PLR signals simultaneously at LE and RE in 27 trials. And we can only carry out CPSD from these 27 trials for assess the PLR signals. From Table 2, we can see that the results of PB are more robust due to larger number of "useful" trials. The time delays in PLR and PB using CPSD method were summarized in Fig. 8.

Appendix B: HbO and Hb

We investigate the relationship between HbO and Hb in 6 sites among 25 people in RS, which was shown in Table 3. As for HbO and Hb in symmetric site, it was shown in Table 4.

Table 3 MCCCs and delays between LFO of [HBO] and [HB] in same site in RS state.

Value	LE	RE	LF	RF	LT	RT
MCCCs	0.6 ± 0.3	0.64 ± 0.11	0.56 ± 0.49	0.48 ± 0.52	-0.11 ± 0.68	-0.15 ± 0.64
Delays (s)	0.6 ± 0.74	0.57 ± 0.46	0.02 ± 0.71	0.6 ± 0.95	0.0032 ± 1	-0.38 ± 1.16

Table 4 Comparisons between calculations from LFO of [HBO]([HB]) component in symmetric site on MCCC and delays in RS state.

	MCCCs		Delays (s)	
Relationship	LFO [HBO]	LFO [HB]	LFO [HBO]	LFO [HB]
LE-RE	0.74 ± 0.14	0.63 ± 0.2	-0.19 ± 0.82	-1.02 ± 2.43
LF-RF	0.92 ± 0.08	0.75 ± 0.19	0.06 ± 0.74	-0.03 ± 3.23
LT-RT	0.89 ± 0.06	0.71 ± 0.2	0.61 ± 0.87	0.22 ± 2.28

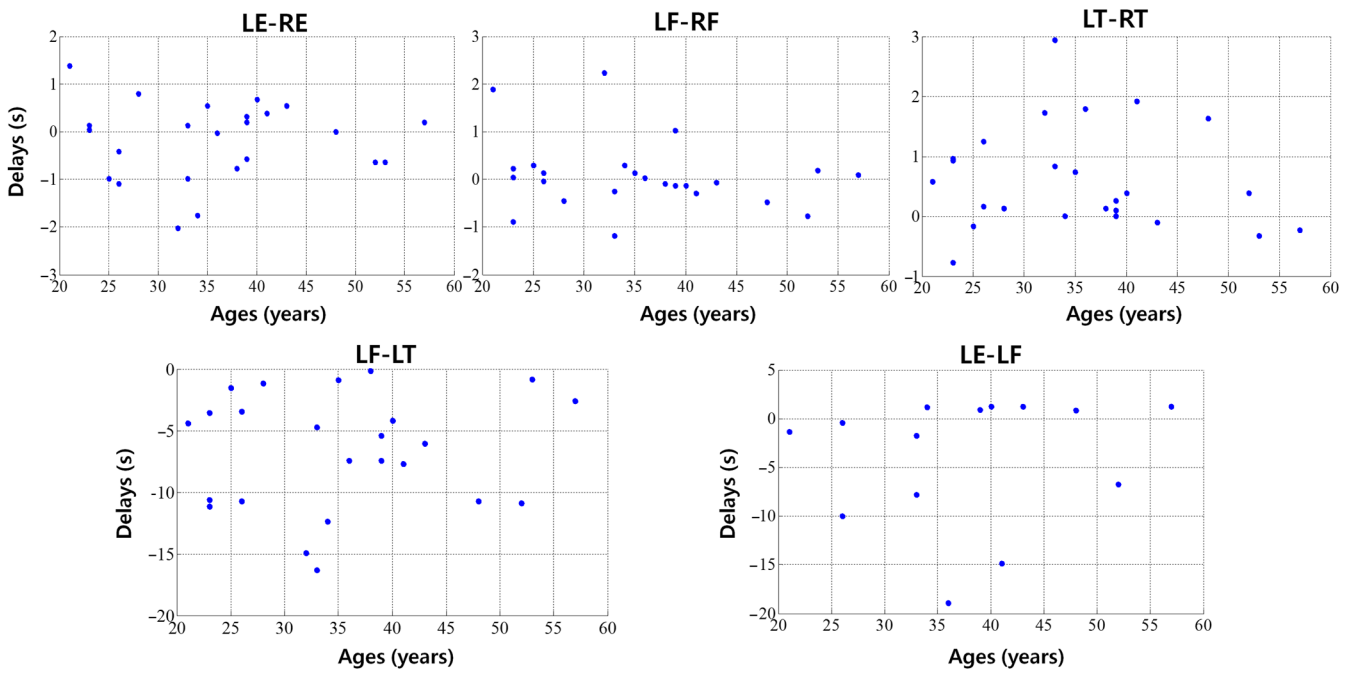

Fig. 9 Time delays with age in five graphs (LE-RE, LF-RF, LT-RT, LF-LT, and LE-LF) in RS among 25 people.

Appendix C: Time Delays with Ages

We also investigate the relationship between time delays and ages in RS state, which is shown in Fig. 9.

Disclosures

The authors have no relevant financial interests in this article and no potential conflicts of interest to disclose.

Acknowledgments

The work was supported by the National Institutes of Health under Grant Nos. K25 DA031769 (Y.T.) and R21 DA032746, R01 NS097512 (B.deB.F). We would like to thank Dr. Zhenhu Liang and Charles F. Babbs, MD, PhD for useful discussion.

References

1. L. N. Livera et al., "Cyclical fluctuations in cerebral blood volume," *Arch. Dis. Child.* **67**(1 Spec No), 62–63 (1992).
2. Y. Hoshi et al., "Relationship between fluctuations in the cerebral hemoglobin oxygenation state and neuronal activity under resting conditions in man," *Neurosci. Lett.* **245**(3), 147–150 (1998).
3. C. E. Elwell et al., "Oscillations in cerebral haemodynamics. Implications for functional activation studies," *Adv. Exp. Med. Biol.* **471**, 57–65 (1999).
4. T. Katura et al., "Quantitative evaluation of interrelations between spontaneous low-frequency oscillations in cerebral hemodynamics and systemic cardiovascular dynamics," *NeuroImage* **31**(4), 1592–1600 (2006).
5. P. Tass et al., "Detection of n:m phase locking from noisy data: application to magneto-encephalography," *Phys. Rev. Lett.* **81**(15), 3291–3294 (1998).

6. F. Zheng, A. Sassaroli, and S. Fantini, "Phasor representation of oxy- and deoxyhemoglobin concentrations: what is the meaning of out-of-phase oscillations as measured by near-infrared spectroscopy?" *J. Biomed. Opt.* **15**(4), 040512 (2010).
7. M. Reinhard et al., "Oscillatory cerebral hemodynamics—the macro- vs. microvascular level," *J. Neurol. Sci.* **250**(1–2), 103–109 (2006).
8. A. V. Medvedev et al., "Event-related fast optical signal in a rapid object recognition task: improving detection by the independent component analysis," *Brain Res.* **1236**(43), 145–158 (2008).
9. K. J. Friston, "Functional and effective connectivity: a review," *Brain Connect.* **1**(1), 13–36 (2011).
10. M. Hampson et al., "Detection of functional connectivity using temporal correlations in MR images," *Hum. Brain Mapping* **15**(4), 247–262 (2002).
11. Y. Tong and B. D. Frederick, "Concurrent fNIRS and fMRI processing allows independent visualization of the propagation of pressure waves and bulk blood flow in the cerebral vasculature," *NeuroImage* **61**(4), 1419–1427 (2012).
12. A. Stefanovska, "Coupled oscillators: complex but not complicated cardiovascular and brain interactions," *Conf. Proc. IEEE Eng. Med. Biol. Soc.* **1**, 437–440 (2006).
13. H. Nilsson and C. Aalkjaer, "Vasomotion: mechanisms and physiological importance," *Mol. Interventions* **3**(2), 79–89 (2003).
14. C. Aalkjær, D. Boedtkjer, and V. Matchkov, "Vasomotion—what is currently thought?" *Acta Physiol.* **202**(3), 253–269 (2011).
15. R. K. Pradhan and V. S. Chakravarthy, "Informational dynamics of vasomotion in microvascular networks: a review," *Acta Physiol.* **201**(2), 193–218 (2011).
16. A. Sassaroli et al., "Low-frequency spontaneous oscillations of cerebral hemodynamics investigated with near-infrared spectroscopy: a review," *IEEE J. Sel. Top. Quantum Electron.* **18**(4), 1478–1492 (2012).
17. I. Tachtsidis et al., "Investigation of cerebral haemodynamics by near-infrared spectroscopy in young healthy volunteers reveals posture-dependent spontaneous oscillations," *Physiol. Meas.* **25**(2), 437–445 (2004).
18. S. Fantini et al., "Cerebral blood flow and autoregulation: current measurement techniques and prospects for noninvasive optical methods," *Neurophotonics* **3**(3), 031411 (2016).
19. J. M. Kainerstorfer et al., "Cerebral autoregulation in the microvasculature measured with near-infrared spectroscopy," *J. Cereb. Blood Flow Metab.* **35**(6), 959–966 (2015).
20. Y. Li et al., "A low cost multichannel NIRS spectrometer for monitoring global physiological hemodynamic fluctuations," in *Society for Functional Near Infrared Spectroscopy Biennial Meeting* (2016).
21. Y. Tong and B. D. Frederick, "Time lag dependent multimodal processing of concurrent fMRI and near-infrared spectroscopy (NIRS) data suggests a global circulatory origin for low-frequency oscillation signals in human brain," *NeuroImage* **53**(2), 553–564 (2010).
22. Y. Tong et al., "Low-frequency oscillations measured in the periphery with near-infrared spectroscopy are strongly correlated with blood oxygen level-dependent functional magnetic resonance imaging signals," *J. Biomed. Opt.* **17**(10), 106004 (2012).
23. D. L. Rutlen, F. J. Wackers, and B. L. Zaret, "Radionuclide assessment of peripheral intravascular capacity: a technique to measure intravascular volume changes in the capacitance circulation in man," *Circulation* **64**(1), 146–152 (1981).
24. J. A. Claassen et al., "Transfer function analysis of dynamic cerebral autoregulation: a white paper from the International Cerebral Autoregulation Research Network," *J. Cereb. Blood Flow Metab.* **36**(4), 665–680 (2016).
25. L. M. Hocke et al., "Comparison of peripheral near-infrared spectroscopy low-frequency oscillations to other denoising methods in resting state functional MRI with ultrahigh temporal resolution," *Magn. Reson. Med.* **76**(6), 1697–1707 (2016).
26. S. Fantini, "A haemodynamic model for the physiological interpretation of in vivo measurements of the concentration and oxygen saturation of haemoglobin," *Phys. Med. Biol.* **47**(18), N249–N257 (2002).
27. H. Watanabe et al., "Hemoglobin phase of oxygenation and deoxygenation in early brain development measured using fNIRS," *J. Waterw. Harbor* **23**, 36–60 (2004).
28. Y. J. Zhang et al., "Detecting resting-state functional connectivity in the language system using functional near-infrared spectroscopy," *J. Biomed. Opt.* **15**(4), 047003 (2010).
29. H. Niu et al., "Resting-state functional connectivity assessed with two diffuse optical tomographic systems," *J. Biomed. Opt.* **16**(4), 046006 (2015).
30. T. Takahashi et al., "Influence of skin blood flow on near-infrared spectroscopy signals measured on the forehead during a verbal fluency task," *NeuroImage* **57**(3), 991–1002 (2011).
31. M. Reinhard et al., "Transfer function analysis for clinical evaluation of dynamic cerebral autoregulation—a comparison between spontaneous and respiratory-induced oscillations," *Physiol. Meas.* **24**(1), 27–43 (2003).
32. J. A. Claassen, B. D. Levine, and R. Zhang, "Dynamic cerebral autoregulation during repeated squat-stand maneuvers," *J. Appl. Physiol.* **106**(1), 153–160 (2009).
33. P. J. Eames, J. F. Potter, and R. B. Panerai, "Influence of controlled breathing patterns on cerebrovascular autoregulation and cardiac baroreceptor sensitivity," *Clin. Sci.* **106**(2), 155–162 (2004).
34. H. Obrig et al., "Spontaneous low frequency oscillations of cerebral hemodynamics and metabolism in human adults," *NeuroImage* **12**(6), 623–639 (2000).
35. D. L. Reich et al., "Trendelenburg position and passive leg raising do not significantly improve cardiopulmonary performance in the anesthetized patient with coronary artery disease," *Crit. Care Med.* **17**(4), 313–317 (1989).
36. M. L. Pierro et al., "Validation of a novel hemodynamic model for coherent hemodynamics spectroscopy (CHS) and functional brain studies with fNIRS and fMRI," *NeuroImage* **85**(2), 222–233 (2014).

Biographies for the authors are not available.